

## Measurements of the Vertical Acceleration in Wind Waves

J. A. EWING, M. S. LONGUET-HIGGINS AND M. A. SROKOSZ

*Institute of Oceanographic Sciences, Wormley, Surrey GU8 5UB, U.K.*

(Manuscript received 18 February 1986, in final form 15 May 1986)

### ABSTRACT

Recent theoretical studies of the accelerations in regular gravity waves of finite steepness have shown striking differences between the Eulerian and the Lagrangian accelerations (those measured by fixed instruments or freely floating instruments, respectively). In the present paper, attention is directed to field observations of accelerations in random seas. Two sets of data are analyzed, representing Eulerian and Lagrangian measurements. The Eulerian accelerations are found to be notably asymmetric, with maximum downwards accelerations exceeding  $-1.6g$ . The Lagrangian acceleration histograms are narrower and more symmetric, in general. As might be expected, the acceleration variance is highly sensitive to the high-frequency cutoff, in both types of data.

### 1. Introduction

Sea surface accelerations are of basic importance to our understanding of surface gravity waves and of the shorter capillary-gravity waves which ride on them. For pure gravity waves it is clear that the ratio of the maximum particle acceleration  $\alpha_{\max}$  to the acceleration of gravity  $g$  is an important measure of the nonlinearity. Various criteria for wave breaking have been proposed in terms of the quantity  $R = |\alpha_{\max}|/g$ . Phillips (1958) suggested the value  $R = 1$ . Snyder and Kennedy (1983) use the value  $R = 0.5$  and Srokosz (1986) has proposed  $R = 0.4$ . In a recent contribution Longuet-Higgins (1985) made a theoretical study of the accelerations in steep gravity waves and pointed out the importance of distinguishing between the apparent (or Eulerian) accelerations that are measured by a fixed wave probe on the one hand, and on the other the real (or Lagrangian) accelerations that are measured by an ideal floating buoy. His conclusions were surprising: for limiting Stokes waves, i.e., waves having a crest angle of  $120^\circ$ , the *apparent* acceleration at the free surface varies between  $0.24g$  (upward) in the wave trough to *minus infinity* at the wave crest. The real, or Lagrangian, acceleration, on the other hand, is much smoother and varies from  $0.30g$  in the wave trough to  $-0.39g$  near the crest.

However, these results do not necessarily apply to *unsteady* gravity waves, or to a mixture of progressive waves. In standing waves, for example, we certainly expect limiting vertical accelerations of  $-g$  (see Taylor, 1955). Moreover, one can construct an example of superposed *progressive* waves in which the downwards Lagrangian acceleration approaches  $-g$  (Longuet-Higgins, 1985).

For oceanographic purposes we are naturally most interested in *random* wave motions, hence those mo-

tions having a more or less continuous spectrum. At the present time, the only available approach is by field observations or by experiments in the laboratory. In this paper we undertake a preliminary examination of wave data obtained by both Eulerian and Lagrangian methods. In section 2 we consider wave measurements taken with fixed wave gauges. In section 3 we describe others taken with wave accelerometer buoys. A discussion, with conclusions, follows in section 4.

### 2. Measurements with fixed instruments

In this section we analyze a set of observations made with vertical capacitance-wires, of diameter 1.4 mm, attached to a fixed platform in the Queen Elizabeth II Reservoir at Hersham, Surrey. The reservoir is roughly pentagonal in shape, with a diameter of 1.5 km. The platform is located in water of depth 20 m, near the southeast corner of the reservoir (see Fig. 1). The wave recorders were attached to the platform by a boom, at a distance of 3 m from the nearest leg of the tower, and open to waves from the north and west. Interference by reflection from the structure of the tower was judged to be negligible.

The reservoir itself has sloping sides, inclined at about  $18^\circ$  to the horizontal, so that reflection at the boundaries was probably small.<sup>1</sup>

There were altogether six capacitance wires in a linear array of total length 3 m aligned in the east-west direction. Normally all instruments were recording simultaneously, and the observations were drawn particularly from wire number 3, at a distance 1.25 m

<sup>1</sup> The work of Moraes (1970) indicates that for actively generated waves with slopes of order 0.05, the reflection coefficient would be between 15 and 20 percent. The reflected waves would be further reduced by an adverse wind.

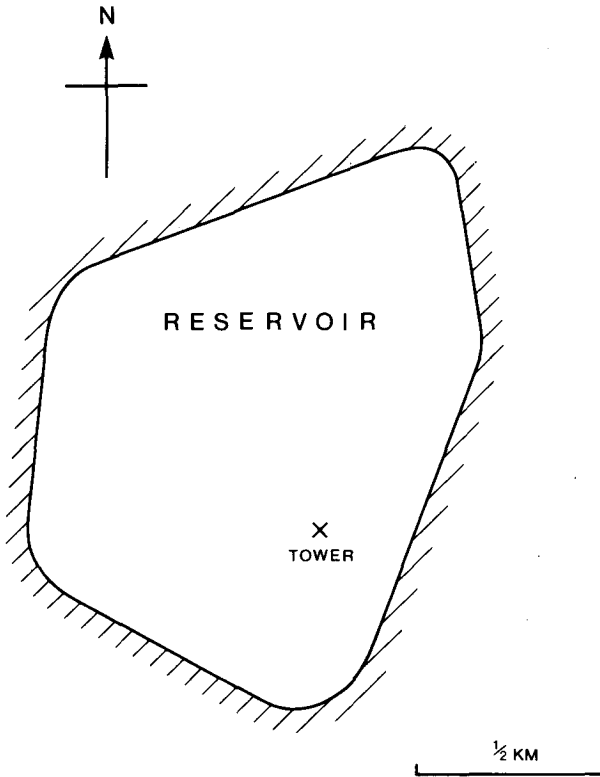


FIG. 1. Plan of the Queen Elizabeth II Reservoir near Hersham, Surrey.

from the western end. The other wires were used for checking and comparison. As expected, there was no systematic difference between the various wave records.

Wind speed and direction were recorded at 10 m height above the mean water level by a standard cup anemometer and vane attached to the platform. In one case this was compared to a hand-held anemometer reading.

We considered five different records, for which the environmental data are given in Table 1. In the last column is the effective fetch  $X$ , which of course depended on the wind direction. The maximum wind speed was  $12.4 \text{ m s}^{-1}$  and the maximum fetch less than 1.1 km.

Each record consisted of 8000 successive digital readings of surface elevation, taken every 0.125 s, the total duration being 1000 s. To calculate the frequency spectra, the first 2048 points of each record were Fourier-analyzed by a standard routine (NAGLIB G13CBF). The resulting spectra  $S(f)$  of surface elevation are shown in Figs. 2a–e. These appear to vary as  $f^{-5}$  over most of the range of interest. Table 2 gives details of the peak frequencies  $f_p$  and of the spectral moments

$$M_r = \int_0^{f_N} f^r S(f) df$$

calculated up to the Nyquist frequency  $f_N = 4.0 \text{ Hz}$ .

To obtain the (apparent) accelerations from each record of the surface elevation, two different methods were tried. In the first, an  $n$ -point interpolation formula was used to fit a polynomial  $Z_n(t)$  of degree  $(n - 1)$  to  $n$  successive data points  $\zeta$ . This polynomial was then differentiated twice to give an estimate  $e_n = d^2 Z_n / dt^2$  of  $\zeta_{tt}$ . To test the accuracy, the standard deviation of  $e_n/g$  was calculated for  $n = 3, 5$  and  $7$  and compared with the value  $m_4^{1/2}/g = 4\pi^2 M_4^{1/2}/g$  derived from the Fourier analysis. These are shown in Table 3. Clearly as  $n$  increases, so the standard deviations approach  $m_4^{1/2}/g$ , but even when  $n = 7$  the differences are still of order ten percent.

Second, the acceleration was calculated by Fourier-transforming the 8000 readings of surface elevation, then multiplying each Fourier component by minus the square of its frequency, and summing the series (i.e., performing the inverse Fourier transform) to get individual estimates, which we denote by  $e_\infty$ . The standard deviation of  $e_\infty/g$  is also shown in Table 3, from which it can be seen to be in quite close agreement with  $m_4^{1/2}/g$ .

From this we can conclude that even a 7-point interpolation formula would significantly underestimate the magnitude of the acceleration, but that the Fourier transform method underestimates it only slightly. We therefore adopted the Fourier transformed estimates as the basis for our discussion.

Histograms of the resulting accelerations  $e_\infty$  normalized by gravity  $g$  are shown in Fig. 3. It can be seen immediately that at the lowest wind speed (record 05) the histogram is fairly symmetric, but that at highest wind speeds (Records 20 and 23) there is a pronounced negative tail. This is borne out by Table 4, where Records 20 and 23 are seen to be associated with a substantially negative coefficient of skewness  $\lambda_3$  and some downward accelerations exceeding  $-1.2g$  in both cases. The upward accelerations never exceed  $0.8g$ .

To illustrate the contribution to the variance  $K_2$  from different parts of the frequency spectrum we show in Fig. 4 a plot of  $fA(f)/g^2$ , where  $A(f) = f^4 S(f)$  is the acceleration spectrum, versus  $\ln f$ . (Because of "aliasing," the spectrum is valid only up to  $f = 3.0 \text{ Hz}$ .) The quantity plotted is a measure of the contribution to the acceleration variance per octave of frequency; the total variance is found by integrating  $fA(f)$  with respect to  $\ln f$ .

TABLE 1. Environmental data for the wave records from the Queen Elizabeth II Reservoir.

| Record | Date (day/mo/yr) | Starting time (GMT) | $U_{10}$ ( $\text{m s}^{-1}$ ) | $\theta$ (deg) | $X$ (m) |
|--------|------------------|---------------------|--------------------------------|----------------|---------|
| 05     | 21/4/82          | 1308                | 3.7                            | 050            | 500     |
| 08     | 21/7/82          | 1343                | 7.1                            | 020            | 1035    |
| 20     | 22/3/83          | 1310                | 12.4                           | 270            | 770     |
| 23     | 24/3/83          | 1229                | 10.8                           | 000            | 920     |
| 45     | 16/4/84          | 1330                | 7.0                            | 310            | 910     |

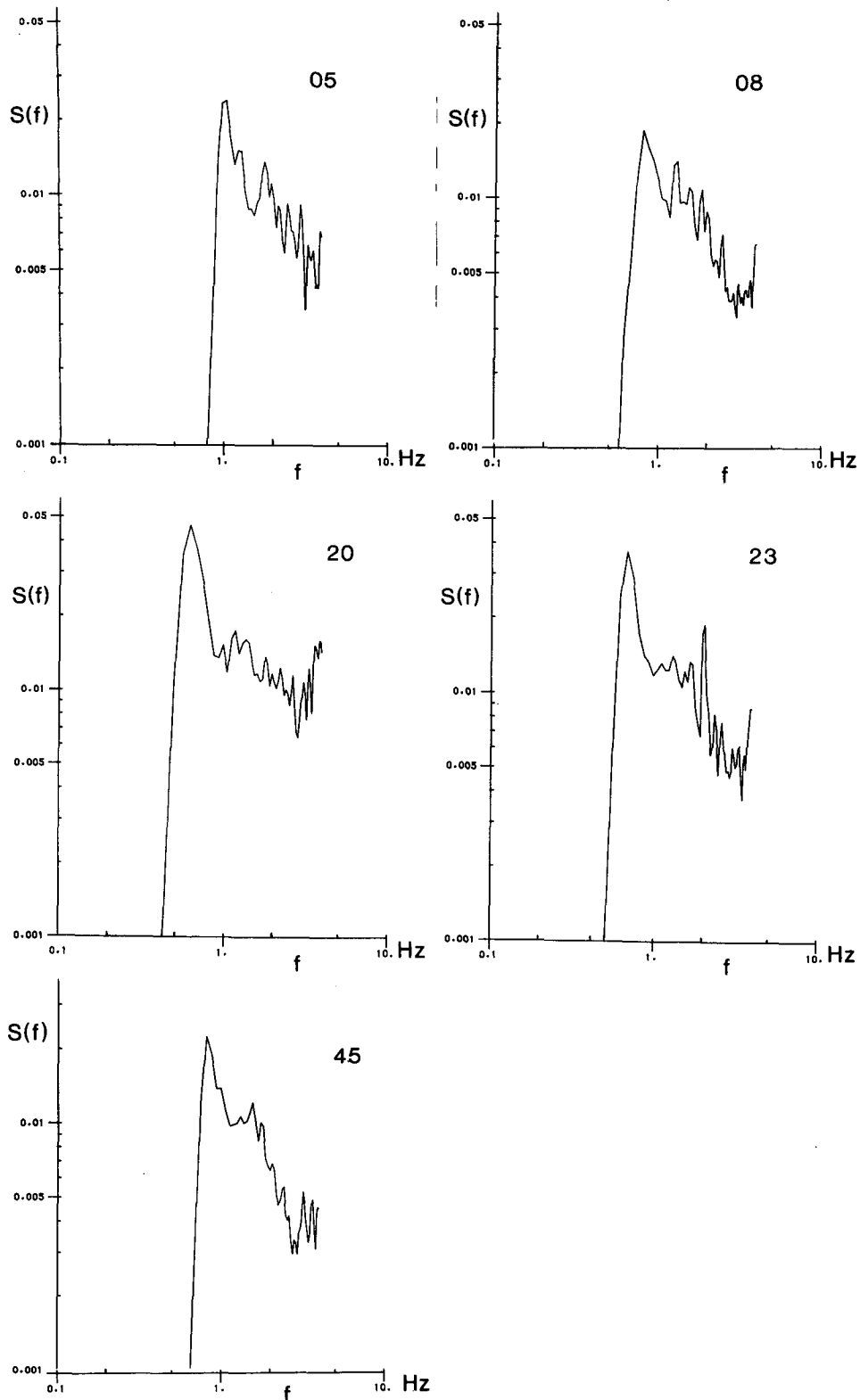


FIG. 2. Frequency spectra  $S(f)$  of the five wave records listed in Table 1.

TABLE 2. Moments  $M_r$  and peak frequencies  $f_p$  for the five wave records listed in Table 1. The units are cm and sec.

| Record | $M_0$ | $M_1$ | $M_2$ | $M_3$ | $M_4$ | $f_p$ |
|--------|-------|-------|-------|-------|-------|-------|
| 5      | 4.83  | 5.42  | 6.90  | 10.1  | 17.5  | 1.01  |
| 8      | 9.40  | 8.45  | 8.63  | 10.4  | 15.7  | 0.80  |
| 20     | 52.8  | 33.3  | 24.9  | 23.5  | 31.9  | 0.59  |
| 23     | 25.6  | 18.8  | 15.8  | 14.7  | 21.8  | 0.67  |
| 45     | 8.73  | 8.08  | 8.38  | 10.1  | 15.1  | 0.81  |

TABLE 3. Standard deviations of the estimated accelerations.

| Record | $\bar{e}_3$ | $\bar{e}_5$ | $\bar{e}_7$ | $\bar{e}_\infty$ | $m_4^{1/2}/g$ |
|--------|-------------|-------------|-------------|------------------|---------------|
| 05     | 0.125       | 0.143       | 0.149       | 0.160            | 0.168         |
| 08     | 0.127       | 0.142       | 0.147       | 0.155            | 0.160         |
| 20     | 0.175       | 0.195       | 0.202       | 0.220            | 0.227         |
| 23     | 0.154       | 0.171       | 0.176       | 0.187            | 0.188         |
| 45     | 0.130       | 0.146       | 0.153       | 0.161            | 0.156         |

As one would expect from the form of the elevation spectra  $S(f)$ , we find that  $fA(f)$  is roughly a constant at frequencies  $f > f_p$ , with the exception of an unexplained peak at 2.1 Hz in Record 23. Generally there is little indication that  $fA(f)$  is decreasing at the upper frequency limit. Our conclusion is that the acceleration variance is strongly dependent on the high-frequency

cutoff, at least under conditions of active wave generation.

### 3. Lagrangian measurements

As typical Lagrangian observations of the vertical acceleration we selected representative wave records made with the pitch-and-roll buoy (Longuet-Higgins

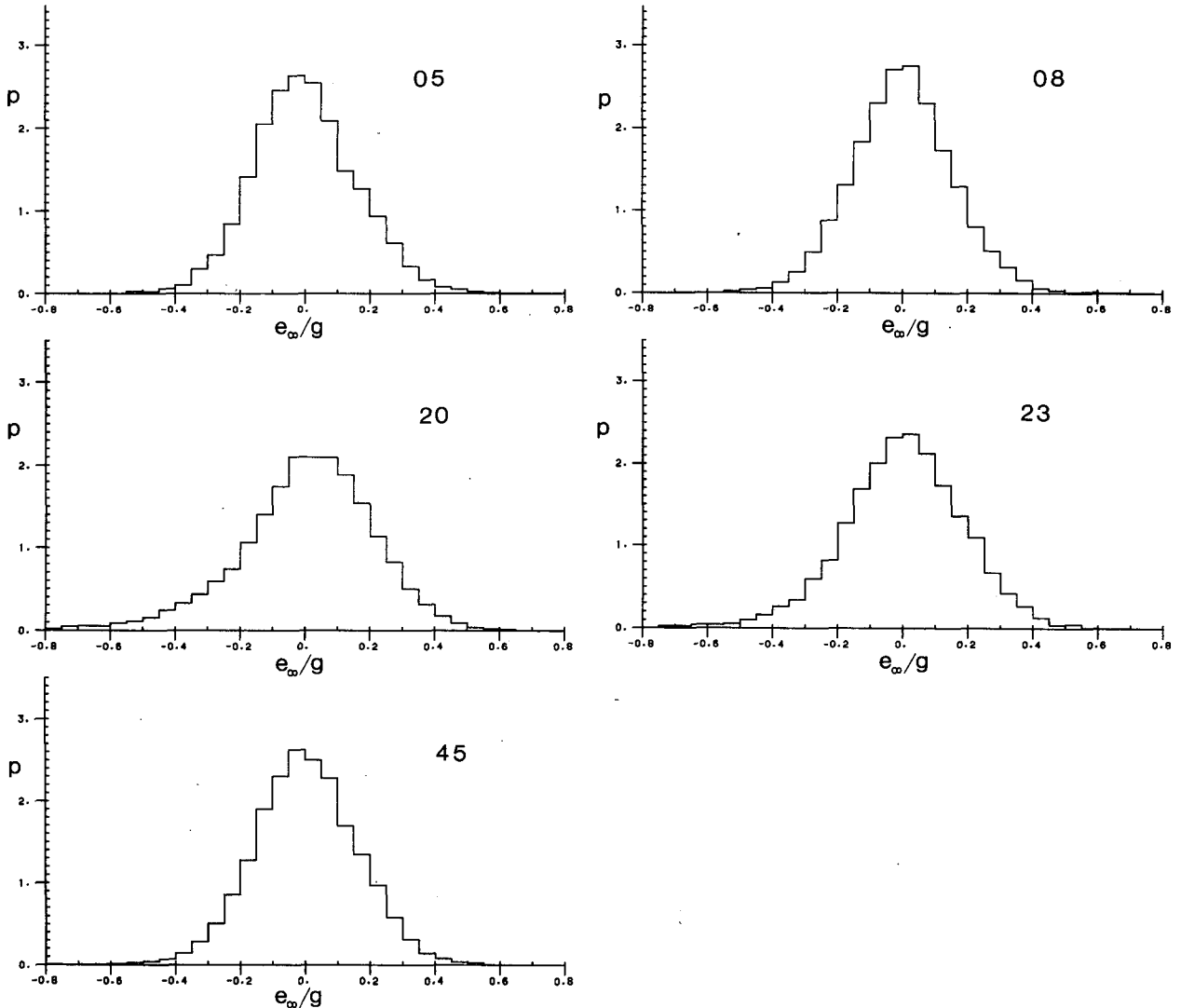


FIG. 3. Histograms of the apparent acceleration  $e_\infty$  derived from the records in Table 1.

TABLE 4. Parameters of the histograms of apparent accelerations  $e_{\infty}/g$  shown in Fig. 3.

| Record | $e_{\infty}/g$ |      | $K_2^{1/2}$ | $\lambda_3$ | $\lambda_4$ |
|--------|----------------|------|-------------|-------------|-------------|
|        | min            | max  |             |             |             |
| 05     | -1.11          | 0.78 | 0.160       | 0.16        | 0.78        |
| 08     | -0.96          | 0.68 | 0.155       | 0.01        | 0.65        |
| 20     | -1.60          | 0.78 | 0.220       | -0.91       | 2.84        |
| 23     | -1.26          | 0.73 | 0.187       | -0.42       | 1.36        |
| 45     | -1.13          | 0.62 | 0.161       | -0.16       | 0.94        |

et al., 1963; Clayton and Smith, 1971). This device is essentially a flat, freely tethered buoy, of overall diameter 1.2 m, carrying a gymbal-mounted, gyro-stabilized accelerometer at its center, whose motions are weakly damped. Effectively, therefore, this instrument measures the vertical component of the orbital acceleration. The frequency response is shown in Fig. 5. There are two curves; one is from an electronic filter, designed to avoid aliasing from energy above the Nyquist frequency. The second theoretical curve in-

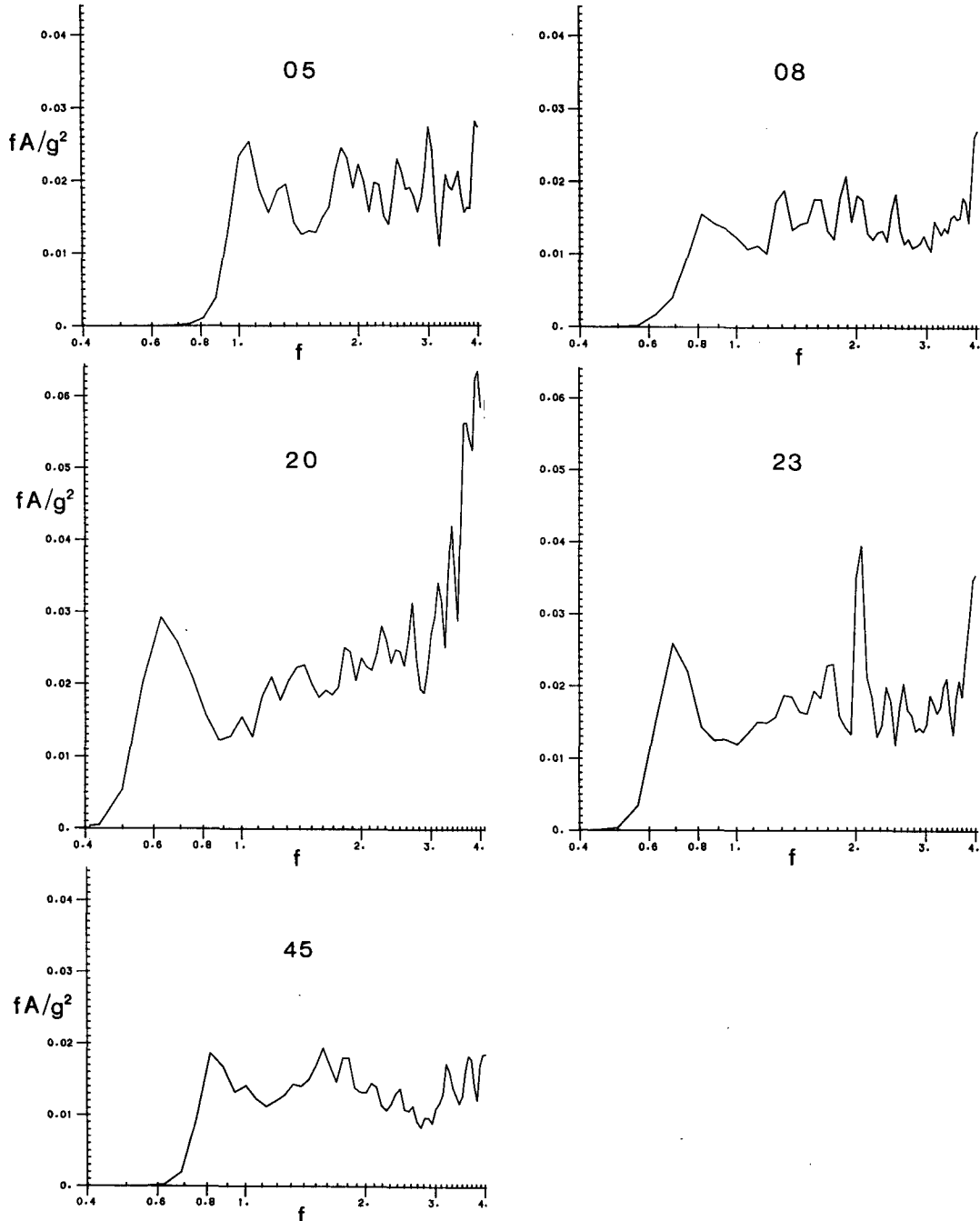


FIG. 4. The dimensionless function  $fA/g^2$  where  $A$  is the spectrum of  $e_{\infty}$ , for each of the records in Table 1.

dicates the damping of the shorter waves by the finite diameter of the pitch-and-roll buoy. The curve is based on the theoretical response to surface waves of a half-immersed ellipsoid of the same horizontal diameter and aspect ratio 0.125 (Kim, 1966).

Environmental details are given in Table 5. The first two records, U01 and U17 were taken off South Uist in the Outer Hebrides (57.3°N, 7.9°W). Of these, the first record represents swell conditions, with a very light wind; the second is an almost pure wind sea. The remaining five records in Table 5 were from Fram Strait in the Norwegian Sea (78.8°N, 1.0°W) during the Marginal Ice Zone Experiment (see Wadhams et al., 1986). The three records M20, M21 and M22 represent a growing wind sea in the presence of some swell. The last two records M30 and M31 are from a similar situation but with a lighter wind.

The corrected acceleration spectra, in the form  $fA(f)/g^2$  versus  $\ln f$ , are shown in Figs. 6a–g. Because of the uncertainty of the buoy response at higher frequencies, these have been plotted only as far as  $f = 0.6$  Hz. After an initial rise, the curves continue either at a constant or increasing level, in each case. This indicates that the spectra of surface elevation decreases no more rapidly than  $f^{-5}$ , and in some cases, particularly U01, U17, M30 and M31, more like  $f^{-4}$ , as far as the spectra are measured. This would be consistent with the observations of Kahma (1981), Donelan et al. (1985) and others. On theoretical grounds Kahma (1981) suggested a transition from  $f^{-4}$  to  $f^{-5}$  behavior at a frequency of order  $2\pi^{-1}g/U_{10}$  which also is not inconsistent with our data, including those in section 2.

In record U01 the very small contribution of the swell at 0.14 Hz to the acceleration variance will be noted, even though this swell largely determines the zero-crossing period  $T_z$  (see Table 5).

The histograms of the measured acceleration are shown in Figs. 7a–h. These, of course, are subject to the response factors of the instrument and so have an effective cutoff at about 0.7 Hz. The parameters of the histograms are given in Table 6. The largest acceleration variance is for U17, corresponding to the highest

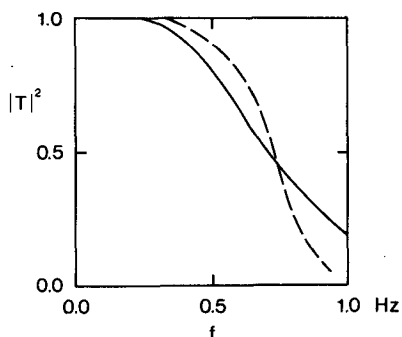


FIG. 5. Response functions for the pitch-and-roll buoy: — electronic filter; --- estimated dynamic response.

TABLE 5. Pitch-and-roll buoy: environmental data.

| Record | Date (day/mo/yr) | Starting time (GMT) | $U_{10}$ ( $m s^{-1}$ ) | $\theta$ (deg) | $H_s$ (m) | $T_z$ (s) |
|--------|------------------|---------------------|-------------------------|----------------|-----------|-----------|
| U01    | 22/7/83          | 1300                | <1.5                    | —              | 2.0       | 7.2       |
| U17    | 27/7/83          | 0400                | 11                      | 340            | 1.7       | 4.8       |
| M20    | 13/7/83          | 1923                | 5                       | 180            | 0.5       | 4.8       |
| M21    | 13/7/83          | 2131                | 6                       | 190            | 0.6       | 4.0       |
| M22    | 13/7/83          | 2300                | 6                       | 195            | 0.6       | 4.2       |
| M30    | 21/7/84          | 0624                | 4                       | 155            | 0.8       | 5.3       |
| M31    | 21/7/84          | 0817                | 4                       | 155            | 0.9       | 5.6       |

wind speed, 11  $m s^{-1}$ . In that case the minimum and maximum accelerations were  $-0.38g$  and  $0.36g$ , respectively. In each of the records there is a notable lack of asymmetry, the coefficient of skewness  $\lambda_3$  being always less than 0.04 in magnitude.

#### 4. Discussion and conclusions

We have analyzed acceleration data from two kinds of sources: fixed capacitance-wire gauges in a reservoir at short fetches, with active wave generation, and free-floating accelerometer buoys, under more varied oceanic conditions. In the first type of situation the acceleration spectrum  $A(f)$  behaved like  $f^{-1}$ , and in the second type it was almost constant over the range of interest. In both cases the acceleration variance depended strongly on the high-frequency cutoff.

In the real (Lagrangian) measurements the acceleration histograms were roughly symmetric; this may be related to the symmetric nature of the Lagrangian accelerations in a regular wave of finite steepness (Longuet-Higgins, 1985). In our data no acceleration much exceeded  $0.4g$  in magnitude, which is approximately the limit for a regular wave.

On the other hand, in the apparent (Eulerian) measurements the histograms became skew at the higher wind speeds, and downward accelerations as great as  $-1.6g$  were recorded. This seems to be a reflection of the strong asymmetry of the apparent accelerations in regular gravity waves and the absence of any limit to the downward acceleration (Longuet-Higgins 1985).<sup>2</sup>

The relation of these results to the incidence of wave breaking is of some interest. Observations in random seas under conditions of wave generation suggest that breaking can take place on a wide range of scales. Like the counting of wave crests, the number of breaking waves per unit time or area of sea surface will depend on the scales considered. For example, for many engineering purposes we are interested only in the larger length-scales, whereas for momentum transfer to currents, the shorter scales may be more important. This scale-dependence of "breaking waves" is paralleled by

<sup>2</sup> Because of the finite spectral bandwidth, the observed maximum and minimum accelerations are regarded strictly as lower bounds.

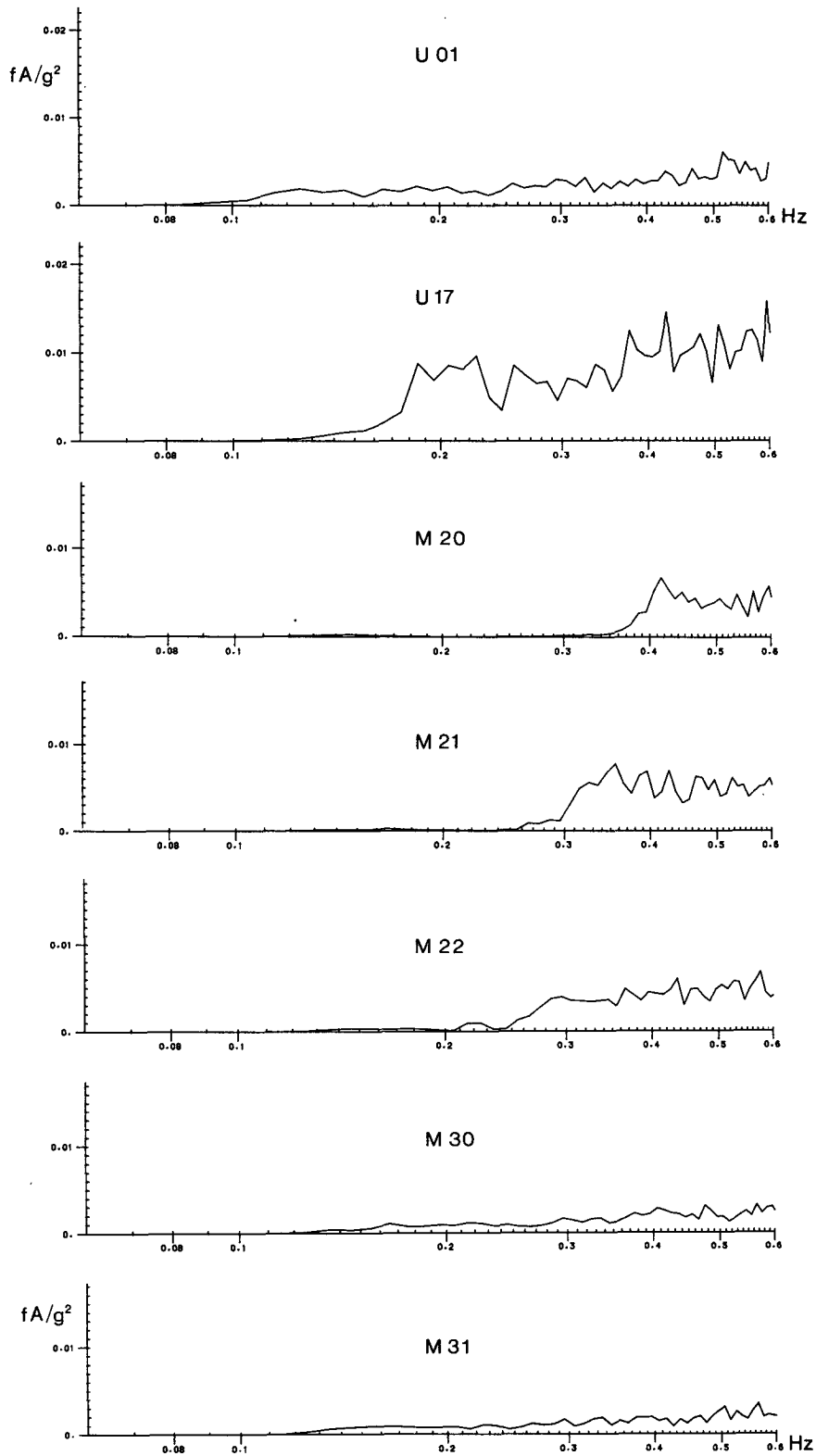


FIG. 6. The dimensionless function  $fA/g^2$ , for each of the pitch-and-roll buoy records.

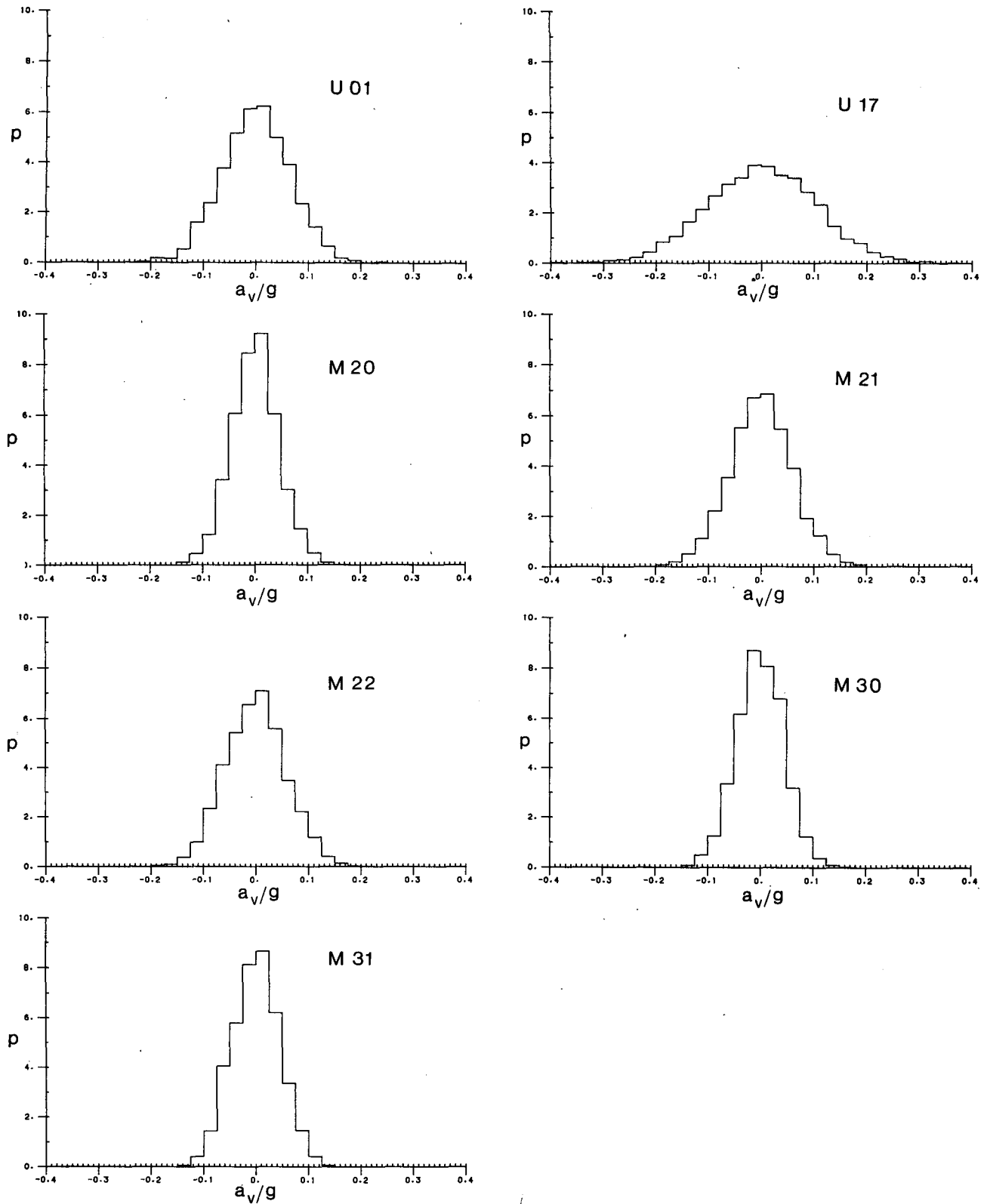


FIG. 7. Histograms of the Lagrangian acceleration for each of the pitch-and-roll buoy records.



TABLE 6. Pitch-and-roll buoy: parameters of the acceleration histograms.

| Record | $a_w/g$ |      | $K_2^{1/2}/g$ | $\lambda_3$ | $\lambda_4$ |
|--------|---------|------|---------------|-------------|-------------|
|        | min     | max  |               |             |             |
| U01    | -0.22   | 0.25 | 0.065         | 0.008       | 0.10        |
| U17    | -0.38   | 0.36 | 0.103         | -0.040      | 0.04        |
| M20    | -0.15   | 0.15 | 0.045         | 0.033       | 0.12        |
| M21    | -0.19   | 0.26 | 0.059         | 0.021       | 0.11        |
| M22    | -0.20   | 0.20 | 0.057         | 0.044       | -0.07       |
| M30    | -0.14   | 0.15 | 0.044         | 0.001       | 0.01        |
| M31    | -0.14   | 0.18 | 0.045         | 0.014       | -0.14       |

the sensitivity of the fourth moment  $m_4$ , hence the ratio  $m_4^{1/2}/g$ , to the high-frequency cutoff, as is well known and as we have verified. In our observations, whether Eulerian or Lagrangian, there were no independent observations of wave breaking. However, in the Eulerian data, at such short fetches, breaking of the dominant waves was probably present, particularly at the higher wind speeds. We note that our data give no support to previous suggestions that in random waves the histogram of the accelerations is limited to some fixed proportion of  $g$ .

REFERENCES

Clayson, C. H., and N. D. Smith, 1971: Recent advances in wave buoy techniques at the National Institute of Oceanography. *Rad. Electron. Eng.*, **41**, 291-301.

Donelan, M. A., J. Hamilton and W. H. Hui, 1985: Directional spectra of wind-generated waves. *Phil. Trans. Roy. Soc. London.*, **A315**, 509-562.

Kahma, K. K., 1981: A study of the growth of the wave spectrum with fetch. *J. Phys. Oceanogr.*, **11**, 1503-1515.

Kim, W. D., 1966: On a free-floating ship in waves. *J. Ship Res.*, **10**, 182-200.

Longuet-Higgins, M. S., 1985: Accelerations in steep gravity waves. *J. Phys. Oceanogr.*, **15**, 1570-1579.

—, D. E. Cartwright and N. D. Smith, 1963: Observations of the directional spectrum of sea waves using the motions of a floating buoy. *Ocean Wave Spectra*. Prentice Hall, 111-136.

Moraes, C. de C., 1970: Experiments of wave reflexion on impermeable slopes. *Proc. 12th Conf. on Coastal Engineering*, Washington, DC, Amer. Soc. Civil Engineers, 509-521.

Phillips, O. M., 1958: The equilibrium range in the spectrum of wind generated waves. *J. Fluid Mech.*, **4**, 426-434.

Snyder, R. L., and R. M. Kennedy, 1983: On the formation of whitecaps by a threshold mechanism. Part 1. Basic formalism. *J. Phys. Oceanogr.*, **13**, 1482-1492.

Srokosz, M. A., 1986: A note on the probability of wave breaking in deep water. *J. Phys. Oceanogr.*, **16**, 382-385.

Taylor, G. I., 1955: An experimental study of standing waves. *Proc. Roy. Soc. London*, **A218**, 44-59.

Wadhams, P., V. A. Squire, J. A. Ewing and R. W. Pascal, 1986: The effect of the marginal ice zone on the directional wave spectrum of the ocean. *J. Phys. Oceanogr.*, **16**, 358-376.